Space Physics Advanced Option on the Solar Wind and Heliosphere – Worksheet Solutions

Dr. R.J. Forsyth, Room 308, r.forsyth@ic.ac.uk

December 2003

1. The size of the heliosphere

(a) Dynamic pressure is given by ρv^2.

Dimensional analysis $\rightarrow$ $kg.m^{-3}.(ms^{-1})^2 \rightarrow kg.m^{-1}.s^{-2}$

Pressure $\equiv$ Force/Area $\rightarrow$ $kg.ms^{-2}.m^{-2} \rightarrow kg.m^{-1}.s^{-2}$

Thus ρv^2 does indeed have the dimensions of a pressure.

(b) Plasma pressure, $P_{plas} = n_p k T_p + n_e k T_e$

Ignoring helium we can take $n_p = n_e$.

Thus $P_{plas} = 10cm^{-3} \times 1.38 \times 10^{-23} JK^{-1} \times (4 \times 10^4 + 1.3 \times 10^5)K$

$= \underline{2.35 \times 10^{-11} Nm^{-2}}$

Magnetic pressure, $P_{mag} = \frac{B^2}{2\mu_0}$

Table 2 only gives us the radial component of the magnetic field at 1AU as 3nT, so let's assume a spiral angle of 45° to allow us to calculate the field strength:

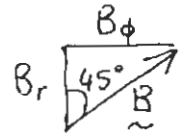

If $B_r = B_\phi = 3nT$ then $|\underset{\sim}{B}| = 4.24\,nT$

and $P_{mag} = \frac{(4.24 \times 10^{-9})^2}{2 \times 4\pi \times 10^{-7}}$

$= \underline{7.15 \times 10^{-12} Nm^{-2}}$

This result is consistent with most of the variability in the solar wind being due to plasma motions ($P_{plas} > P_{mag}$). However it only

needs the magnetic field to increase to ~8 nT (with no other effect) to make them comparable. Thus P_{mag} can occasionally exceed P_{plas} in the solar wind, e.g. in the low β part of transient wind streams.

Dynamic pressure, $P_{dyn} = \rho v^2$

$= n(m_p + m_e)v^2 \quad (m_e \ll m_p)$

$= 10\,cm^{-3} \times 1.67 \times 10^{-27}\,kg \times (400\,kms^{-1})^2$

$= \underline{2.67 \times 10^{-9}\,Nm^{-2}}$.

This is about 2 orders of magnitude bigger than the other two pressures so we can assume that it dominates. With the given assumptions the dynamic pressure will fall off with distance from the Sun following an inverse square law. So with r measured in A.U. we have

$$P_{dyn}(r) = \frac{2.67 \times 10^{-9}}{r^2}\,N\,m^{-2}$$

(c) Now for the interstellar medium:

Plasma pressure $\approx 0.3\,cm^{-3} \times 1.38 \times 10^{-23} \times 7 \times 10^3\,K$

$\approx \underline{5.80 \times 10^{-14}\,Nm^{-2}}$

Assuming an uncertainty of $0.1\,cm^{-3}$ in n_p and $2 \times 10^3\,K$ in T_p gives an error in $P_{plas} \sim \pm 2.5 \times 10^{-14}\,Nm^{-2}$ using standard combination of errors formulae.

Magnetic pressure: assume $|\underline{B}| \approx 0.3 \pm 0.2\,nT$

$$P_{mag} \approx \frac{(0.3 \times 10^{-9})^2}{2 \times 4\pi \times 10^{-7}} = \underline{3.58 \times 10^{-14}\,Nm^{-2}}$$

$(Error \approx 1.20 \times 10^{-14}\,Nm^{-2})$

Dynamic pressure: $\rho V^2 = n_p m_p V^2$

$\approx 0.3\,cm^{-3} \times 1.67 \times 10^{-27}\,kg \times (25\,kms^{-1})^2$

$\approx \underline{3.13 \times 10^{-13}\,Nm^{-2}}$

With uncertainty in $n_p \sim 0.1\,cm^{-3}$ and $V \sim 2\,kms^{-1}$ we get an uncertainty in P_{dyn} of $\sim \pm 1.1 \times 10^{-13}\,Nm^{-2}$

We cannot ignore any of these three pressure contributions in the interstellar medium.

(d) Equating the dynamic pressure in the solar wind to the ~~total~~ pressure in the interstellar medium gives:

$$\frac{2.67 \times 10^{-9}}{r^2} = 4.07 \times 10^{-13}\,Nm^{-2} \quad (r \text{ in AU})$$

$$\Rightarrow r = \sqrt{\frac{2.67 \times 10^{-9}}{4.07 \times 10^{-13}}} = \underline{81\,AU}$$

This would imply that Voyager 1 should have reached the outer boundary of the heliosphere this year — which it hasn't unless they are keeping it quiet!

What's our uncertainty? With $r = \sqrt{\frac{2.67 \times 10^{-9}}{P_{ISM}}}$

we have $\delta r = \frac{1}{2}\sqrt{2.67 \times 10^{-9}} \cdot P_{ISM}^{-3/2} \cdot \delta P_{ISM}$

which with $\delta P_{ISM} \approx 1.2 \times 10^{-13}\,Nm^{-2}$ gives $\underline{\delta r \approx \pm 12\,AU}$

Some more recent sources quote much lower values for the plasma density in the interstellar medium which would help move our estimated distance to the termination shock or heliopause outwards.

2. On the Parker spiral model of the heliospheric magnetic field. (4)

(a) For spiral angle ψ

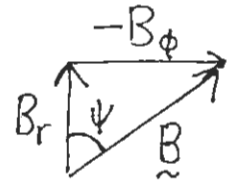

$$\tan\psi = -\frac{B_\phi}{B_r}$$

$$= \frac{B_r(r_\circ,\theta,\phi_\circ)\,\Omega\sin\theta\,.\,r_\circ^2}{V_r\,r}\cdot\left(\frac{r^2}{r_\circ^2}\right)\cdot\frac{1}{B_r(r_\circ,\theta,\phi_\circ)}$$

$$= \frac{\Omega r\sin\theta}{V_r}$$

At 1 AU, $r \sim 1.5\times10^8$ km

$\Omega = 2\pi/T = 2\pi/(86400\times26) = 2.8\times10^{-6}$ rad s^{-1}

At the equator $\theta = 90^\circ \Rightarrow \sin\theta = 1$

Thus $\tan\psi = 2.8\times10^{-6}\,\dfrac{r}{V_r}$

Putting in numbers we get...

At 1 AU for 400 km s^{-1} $\psi = 46.4^\circ$

800 km s^{-1} $\psi = 27.7^\circ$

At 5 AU for 400 km s^{-1} $\psi = 79.2^\circ$

800 km s^{-1} $\psi = 69.1^\circ$

(b) We begin from $\nabla\times\underset{\sim}{B} = \mu_\circ\underset{\sim}{j} \Rightarrow \underset{\sim}{j} = \frac{1}{\mu_\circ}\nabla\times\underset{\sim}{B}$

$$(\nabla\times\underset{\sim}{B})_r = \frac{1}{r\sin\theta}\frac{\partial}{\partial\theta}(B_\phi\sin\theta) - \cancel{\frac{1}{r\sin\theta}\frac{\partial B_\theta}{\partial\phi}} \quad \text{since } B_\theta = 0$$

$$= \frac{1}{r\sin\theta}\frac{\partial}{\partial\theta}\left(-\frac{B_{ro}\Omega\sin^2\theta\, r_\circ^2}{V_r\,r}\right)$$

$$= -\frac{B_{ro}\Omega r_\circ^2}{V_r r^2\sin\theta}\frac{\partial}{\partial\theta}(\sin^2\theta)$$

$$= -\frac{2B_{ro}\Omega r_o^2 \cancel{\sin\theta}\cos\theta}{V_r r^2 \cancel{\sin\theta}}$$

$$(\nabla\times\underset{\sim}{B})_\theta = \frac{1}{r\sin\theta}\frac{\partial B_r}{\partial\phi} - \frac{1}{r}\frac{\partial}{\partial r}(rB_\phi)$$

$= 0$ since B_r is independent of ϕ and B_ϕ goes as $\frac{1}{r}$ so that rB_ϕ is constant.

$$(\nabla\times\underset{\sim}{B})_\phi = \frac{1}{r}\frac{\partial}{\partial r}(rB_\theta) - \frac{1}{r}\frac{\partial B_r}{\partial\theta}$$

$= 0$ since $B_\theta = 0$ and B_r is independent of θ.

Thus we are left with

$$j_r = \frac{1}{\mu_o}(\nabla\times\underset{\sim}{B})_r = -\frac{2B_{ro}\Omega r_o^2\cos\theta}{V_r\mu_o r^2}$$

(c) (i) N. hemisphere, $\underset{\sim}{B}$ outwards $\Rightarrow B_{ro}$ is +ve

$0° < \theta < 90° \Rightarrow \cos\theta$ is +ve

Thus j_r is -ve, and the current flow is inwards.

(ii) S. hemisphere, $\underset{\sim}{B}$ inwards $\Rightarrow B_{ro}$ is -ve

$90° < \theta < 180° \Rightarrow \cos\theta$ is -ve

Thus j_r is again -ve and the current flow is inwards.

(d) $$k_r = \frac{2B_{ro}\Omega r_o^2}{\mu_o V_r r}, \quad k_\phi = \frac{2B_{ro}r_o^2}{\mu_o r^2}$$

With $k_\phi \propto \frac{1}{r^2}$ and $k_r \propto \frac{1}{r}$ the current streamlines form reciprocal spirals as drawn (badly) in the sketch overleaf.

In fact, at any point in the current sheet, $\underset{\sim}{k}$ should be $\perp^{er}$ to $\underset{\sim}{B}$

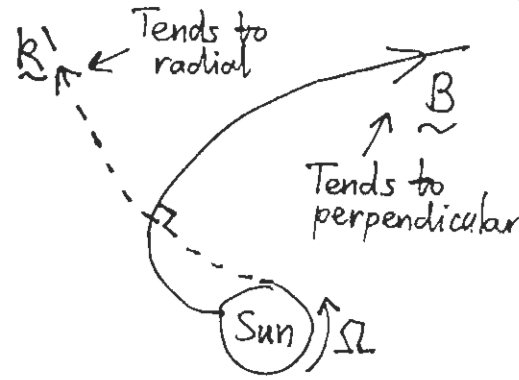

Since k_r and k_ϕ are both +ve the current flow is outwards.

For everything to be OK we will need the outward current flow within the heliospheric current sheet to match the inward volume current flow in the rest of the heliosphere, with the match taking place at the heliopause boundary.

(e) Total current flowing inwards

$$= 2\int_0^{2\pi}\int_0^{\pi/2} j_r r^2 \sin\theta \, d\theta \, d\phi$$

$$= -\frac{4 B_{ro} \Omega r_o^2 \cancel{r^2}}{\mu_o V_r \cancel{r^2}} \int_0^{2\pi}\int_0^{\pi/2} \cos\theta \sin\theta \, d\theta \, d\phi \qquad \left(\int_0^{2\pi} d\phi = 2\pi\right)$$

$$= -\frac{8\pi B_{ro} \Omega r_o^2}{\mu_o V_r} \int_0^{\pi/2} \frac{1}{2} \sin 2\theta \, d\theta \qquad (\sin 2\theta = 2\sin\theta\cos\theta)$$

$$= -\frac{4\pi B_{ro} \Omega r_o^2}{\mu_o V_r} \left[-\frac{1}{2}\cos 2\theta\right]_0^{\pi/2}$$

$$= -\frac{4\pi B_{ro} \Omega r_o^2}{\mu_o V_r}$$

Total current flowing outwards (only radial component k_r will contribute)

$$= \int_0^{2\pi} k_r \, r \, d\phi$$

$$= \frac{2 B_{r_0} \Omega r_0^2}{\mu_0 V_r} \int_0^{2\pi} \frac{r}{r} \, d\phi$$

$$= \frac{4\pi B_{r_0} \Omega r_0^2}{\mu_0 V_r}$$

Adding these two contributions together we find a net current of zero flowing out from the Sun.

3. Interpreting real space physics data...

(a) Forward Shock (FS) The compression region of the CIR can be easily identified as the high pressure region in the lower panel of Figure 1. The pressure gradient at the leading edge of the event is discontinuous indicating that the forward propagating pressure wave has steepened into a forward shock wave. The density, temperature and magnetic field strength all rise discontinuously at the FS and these parameters all contribute to the total pressure. We also have a speed increase at the FS since the forward shock acts to accelerate the slow wind ahead of the interaction region.

Heliospheric Current Sheet (HCS) Following the information in section 2.2 we would expect a HCS crossing to be identified by a 180° change in the magnetic field direction. This is clearly the case in the Φ_B angle in the second to bottom panel in Figure 1.

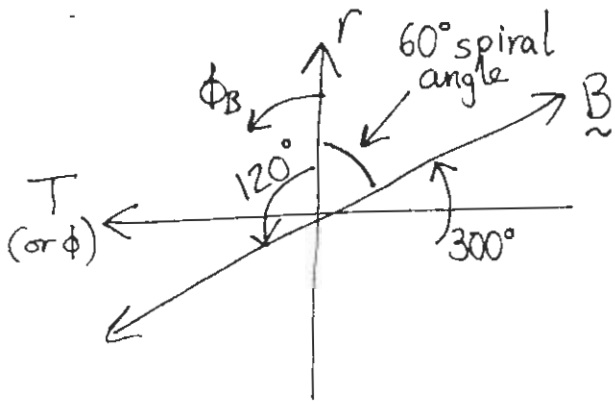

Looking more closely, the azimuth angle ϕ_B changes from ~300° to ~120°. This would correspond (see diagram) to a Parker spiral angle of ~60°. $\phi_B \sim 120°$ corresponds to sunward directed magnetic field while $\phi_B \sim 300°$ corresponds to an outward directed magnetic field. Note $\theta_B \sim 0°$ as predicted by Parker's magnetic field model.

Stream Interface (SI) This is the boundary between the two separate plasmas which started off as slow and fast near the Sun. The most common means of identifying this boundary comes from comparing the proton density and temperature characteristics of the fast and slow wind in Table 2. The fast wind is inherently less dense and hotter than the slow wind. Thus we would expect a density decrease and a temperature increase at the SI. This is the case at the boundary marked on Figure 1, although there is another similar boundary in this CIR less than a day later, indicating that this method is not foolproof. In fact helium and heavier ion composition measurements of the solar wind (not shown here) provide a more robust separation of the two types of wind.

Reverse Wave (RW) This is where the pressure in the lower panel of Figure 1 drops again at the end of the compression region. However, the decrease is not discontinuous here, indicating that the reverse wave has not steepened into a shock. One reason in this example might be that the ambient pressure

behind the interaction region is higher than that in front of it, resulting in a lesser pressure gradient. As in the FS case, we see that the density, temperature and field strength all drop at the RW, consistent with the decrease in pressure. Remembering that the RW is propagating back into the fast wind behind the interaction region, we can interpret the speed increase seen across the RW in the top panel as being consistent with the RW acting to decelerate wind that was previously fast.

(b) Referring to Figure 3.1, we would expect the HCS to lie in the centre of the band of slow solar wind in the ideal case. In a CIR we need to remember that all the solar wind which lies between the FS and the SI was originally slow when it left the Sun. Thus, what has happened here is that the forward wave/shock propagating ahead of the CIR has overtaken that part of the slow wind containing the HCS, accelerating the slow wind as it goes, so that the HCS now lies in the region of compressed plasma constituting the CIR.

(c) I guess 'no' would have been a valid answer here, although you may have written down some features I've already covered above. Although I didn't ask you to, with a little thought you might have been able to explain the behaviour of the V_T component of the solar wind velocity. This is the component of the velocity in the direction perpendicular to the radial direction and lying in the equatorial plane (V_ϕ if we were using spherical polars). T (and ϕ) are positive in the direction of solar rotation. In the two dimensional picture of Figure 3.4 we can see that the compression

region adopts a spiral configuration. Thus, rather than being radial as in our one dimensional discussion, the pressure gradients will have directions as shown by the large white arrows on Figure 3.4. As a result the pressure waves do not propagate purely radially and hence introduce azimuthal (or ϕ) components into the solar wind flow. Inspection of Figure 3.4 suggests that this component should be in the positive T direction for the forward wave and in the negative T direction for the reverse wave, in agreement with the V_T profile in Figure 1. We can see that the V_T deflections reverse at the SI which is consistent with the above argument and gives another means of identifying the SI from solar wind data. To understand the V_N (north-south) component behaviour, similar arguments can be used but it requires moving to a three dimensional viewpoint which is beyond our scope here.

d) Now looking at the transient wind stream in Figure 2.

Upstream Signatures Using the bidirectional electron (BDE) signature as a marker for plasma that was part of the original mass ejection from the Sun, we can see that for ~18 hours ahead of the start of the BDE there are other signatures which arise due to the interaction of the ejecta with the solar wind ahead of it. The discontinuous rise in field strength, speed, density (less so), and temperature early in day 74 are suggestive of a forward shock wave propagating ahead of the event. This requires that an 'interaction region' has developed in front of the ejecta, confirmed by the high field strength,

density and temperature, and hence total pressure, indicating that the plasma is compressed between the FS and the start of the BDE. Note that the front of the ejecta is travelling at ~550 kms^{-1}, ~100kms^{-1} faster than the ambient solar wind ahead. As for the CIR, the FS has acted to accelerate the originally slower wind up to a similar speed to the ejecta in the so-called 'sheath' region which leads the ejecta.

Signatures within the ejected plasma In the region characterised by the BDE, i.e. within the ejected plasma, we can identify a slow rotation of the magnetic field direction, particularly in the θ_B angle. This is suggestive of a coiled magnetic field structure such as that illustrated in the lower panel of Figure 3.6.

The declining solar wind speed as the ejecta crosses the spacecraft suggests that in this example the radial size of the ejecta is expanding as it travels out from the Sun.

The low density and temperature, coupled with the relatively high field strength, suggest that this is a low β plasma, thus helping to preserve the magnetic field structure as it propagates out from the Sun.

Other signatures in Figure 2

HCS crossing You may have noted the 180° change in ϕ_B just behind the FS in this event. As in Figure 1, this marks an HCS crossing that has been 'swept up' into the compression region by the forward shock wave.

Signatures behind the ejecta. The further discontinuous increases in field strength, density, speed and temperature at the end of the BDE region suggest the arrival of another forward shock wave — this is almost certainly due to a further coronal mass ejection causing a transient stream which has caught up with the event we have just been discussing. 1991 was just past the previous solar maximum, so that mass ejection events were relatively frequent at this time.